Proceedings of the 2004 IEEE
International Conference on Robotics & Automation
New Orleans, LA • April 2004

Walking Control of the Humanoid Platform KHR-1 based on Torque Feedback Control

Jung-Hoon Kim and Jun-Ho Oh
Machine Control Laboratory, Department of Mechanical Engineering, KAIST
373-1, Guseong-dong, Yuseong-gu, Daejeon, 305-701, South Korea
E-mail : maysmile@kaist.ac.kr , junhoh@ohzlab.kaist.ac.kr

***Abstract*—This paper presents three online controllers for maintaining dynamic stability of a humanoid robot using force/torque sensor. Those are damping controller, landing orientation controller and landing position controller. The legs of a humanoid robot are relatively long and serially connected with compliant force/torque sensor at the ankle. This architecture has the inherent characteristics of a lightly damped system. Most research on balance control overlook the deterministic vibration caused by structural compliance. In addition, the vibration was not positively considered to improve the characteristics of the system. Therefore, a simple inverted pendulum model with compliant joint is proposed. For this model, the damping controller that increases system damping is proposed as a balance controller. Furthermore, the performance of maintaining balance against external forces is experimentally shown. A landing orientation controller at the ankle joints is presented to manage fast and stable ground contact. A landing position controller is implemented in order to modify the prescribed trajectory of the swing foot and to reduce the landing impact during unexpected landing. The effectiveness of the proposed controllers is confirmed by walking experiments that has been applied on the KAIST humanoid robot platform KHR-1.**

Keywords; Biped humanoid robot; dynamic walk; balance control; damping control; inverted pendulum

I. INTRODUCTION

Biped robots have good mobility in various environments such as rough terrain and stairs. Mobility is very important in the sense that future service robot should help and cooperate with humans in all environments. The demand for developing control algorithm of biped locomotion is increasing, but it is not a simple problem. The biped robot has unstable, nonlinear, and multi-variable dynamics. In addition, the biped robot needs to interact with complex environments. Biped walking is made up of the periodic phase changes between single support and double support. From a viewpoint of system response in one phase, we can say that there is no steady state and only transient state exists. Moreover, the initial condition changes in every transition. Because of the complex nature of dynamic walking, it is meaningful to actually implement the control algorithm experimentally on the robot rather than by simulation alone. So, we developed the humanoid robot platform KHR-1 as a platform for the realization of dynamic walking.

Recently, research on humanoid robots has been increasing since the successful results of Honda R&D, Waseda University, Tokyo University [1-4]. In many cases, the strategies for the walking motion control can be classified into the walking pattern generation related to the motion planning [4-8] and online balance control [1, 9-14]. Walking pattern is generated to ensure that the Zero Moment Point (ZMP) of the robot is inside the supporting foot at all times. This is necessary for the robot to maintain the dynamic stability during bipedal walking [15]. However, the desired ZMP of the walking pattern is different from the actual ZMP of the biped robot during actual walking. In order to compensate for the ZMP error, it is necessary to implement the balance control using force/torque (F/T) sensor or inclination sensor. Several methods of online balance control have been proposed. Some research group realized successful dynamic walking experimentally with their own balance control scheme [1, 8, 11, 12, 14]. Kajita *et al.* introduced a balancing control using direct feedback control of the total angular momentum and the position of the center of gravity [13]. Kāgami *et al.* developed AutoBalancer [14], which modifies the original input trajectories based on many criteria of stability, but Sugihara *et al.* commented that it was hard to apply for the fast dynamic motions because of the complexity of the algorithm and the criteria themselves [16]. Huang *et al.* focused on the generation of smooth walking pattern and their real-time modification contains somewhat rough control equation without mathematical model [17]. Other researchers proposed other balancing method by simulation to improve the computation time and performance [16, 18]. Most researches on the balance control concentrate on the compensation of ZMP error because ZMP is the criteria for the dynamic stability. In many case, it has been assumed that the main cause of the error arises from the unexpected ground condition or model inaccuracy. It is a matter of course that the balance controller should be robust for the inclination and the inaccuracy. However, by observing the experimental result of the position control during single support phase, we noticed that the compliance near ankle joint mainly introduced the ZMP error. The compliance results from the relatively long leg that is serially connected with compliant F/T sensor at the ankle. In most research, the deterministic vibration has been overlooked in the balance control and was not positively considered to improve the characteristics of a lightly damped structure.

In this paper, we propose a simple inverted pendulum model with compliant joint during single support phase, and design a damping controller as a balance controller that improves the damping capability of the system. Its performance of damping out the inherent vibration is experimentally shown. Besides this, we present the landing orientation controller that makes a smooth and fast touchdown of swing leg without resistance. The damping controller and the landing orientation controller are alternated between every phase transition. A landing position controller is also implemented because the unexpected touchdown needs the modification of the foot position in the vertical and horizontal directions. The modification are such that the moment between the two feet and the impact force are altered to maintain stability of the robot. Consequently stable walking could be realized by experiment with these three controllers.

II. Humanoid Robot Platform Description

A. *Mechanical Structure*

The KHR-1 is shown in Fig.1. The total weight, including batteries, computer, controllers and amplifiers, is 48 kg and its height is about 120 cm. The KHR-1 has 21 DOF. Each leg has 6 DOF and it can imitate human walking motion in the sagittal and the frontal plane. The dimension and the D.O.F of KHR-1 are shown in Table 1. The KHR-1 was designed to have a kinematically simple structure. Complicate mechanical design such as differential mechanism was avoided. Harmonic drive gears were used as main reduction gears. Pulley-belt and bevel gear were also used for transmission. The actuators and reduction gears of the lower limbs were selected by introducing a simple model and simulating specific motion patterns in the sagittal and frontal plane [19, 20]. Based on the simulation results, appropriate motor specifications and reduction ratios were selected.

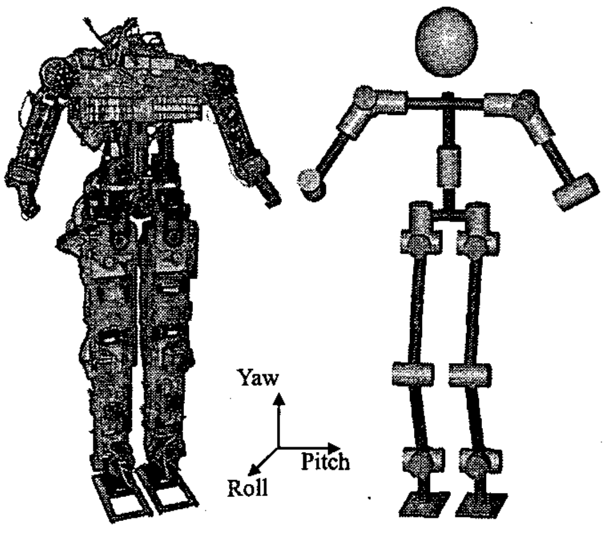

Figure 1. Photograph and joint structure of KHR-1

TABLE I. Specification of Humanoid Robot

Weight	Total	48 kg
Dimension	Height (without head) Width Depth Length of upper arm Length of upper leg Length of lower leg	1193 mm 484 mm 230 mm 255 mm 340 mm 305 mm
Weight	Arms Waist Legs Total	Shoulder 3 D.O.F × 2 Elbow 1 D.O.F × 2 1 D.O.F(Yaw) Hip 3 D.O.F × 2 Knee 1 D.O.F × 2 Ankle 2 D.O.F × 2 21 D.O.F

B. *Hardware architecture*

Fig. 2 shows the overall block diagram of the robot controller. A Pentium III-500 embedded computer with PC104 interface is used as a master controller. It interfaces with two peripheral interface boards (PIB) that can control 12 DC motors. We developed a F/T sensor that can measure two moments up to 34Nm along roll and pitch axes and one normal force up to 95kgf in the vertical direction. It was mounted to the sole of a foot to measure the actual ZMP. The electronic circuit of F/T sensor has a built-in microcontroller (TMS320F241), which transmits the measured signal to the master controller via RS-232 communication at 100Hz. A master controller generates joint commands at 100Hz based on this sensory signal. A linear interpolation of digital PD controllers for DC servo motor is running in the background at 1KHz. An 8-channel A/D converter is used to read analog signals from additional sensors such as rate gyro and accelerometer, etc. In this study, we will focus on sensory feedback using only a F/T sensor. After maximizing the performance with minimum sensor, we will improve the performance with additional sensors in the future research.

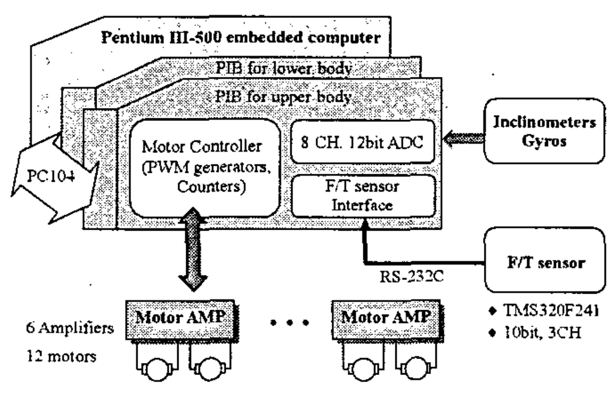

Figure 2. Hardware Architecture

III. Damping Controller at Ankle Joint

A. Simple Inverted Pendulum Model with Compliant Joint

As a model of bipedal walking during single support phase, inverted pendulum model, flywheel model and acrobat model can be assumed [21]. The link is generally assumed to be rigid in many cases, but in a real situation, it is flexible because the foot is connected with a compliant F/T sensor and the leg length is relatively long compared to its cross section. Due to this compliance, the humanoid robot exhibits the characteristics of a lightly damped structure. For example, during the single support phase when the ankle is under position control, the external force will easily excite a sustained oscillation. The oscillation exists even when the position error is nearly zero. When this inherent oscillation occurs, position control of biped walking cannot succeed even if the exact trajectory that satisfies the desired reference ZMP is known. This phenomenon is even prevalent in the fast gait. Therefore, it is desirable to perform the position control considering the stiffness of links using torque feedback. In this paper, a single mass inverted pendulum with compliant joint is considered as the suitable model as shown in Fig. 3 where u denotes the ankle joint angle and θ denotes the actual inclined angle produced by the compliance. The output y is the torque T from the F/T sensor. From the model shown in Fig.3, the equation of motion is derived as

$$y = T = mg\theta - ml^2\ddot{\theta} \quad (1)$$

$$y = K(\theta - u) \quad (2)$$

The transfer function from the ankle joint angle to the torque is derived from the above two equations. [22]

$$\frac{y}{u} = \frac{T}{u} = K\frac{-s^2 + \frac{g}{l}}{s^2 + (\frac{K}{ml^2} - \frac{g}{l})} = K\frac{-s^2 + (\beta - \alpha)}{s^2 + \alpha} \quad (3)$$

where $\alpha = \frac{K}{ml^2} - \frac{g}{l} > 0$, $\beta = \frac{K}{ml^2}$, K is the stiffness of the leg, g is gravity, l is the length of pendulum, and m is the mass, respectively.

If the damping coefficient C of the joint is considered, the torque in (2) can be expressed as $T = K(u - \theta) + C(\dot{u} - \dot{\theta})$. However, for simplicity, the damping coefficient is neglected in this paper, since its value is relatively small compared to the stiffness. The ankle joint angle u is generated by the reference command u_{ref} in the PD position feedback configuration. The transfer function T/u_{ref} has similar dominant poles and zeros with T/u of (3), and also has negligible fast poles over 600 rad/s which correspond to the motor dynamics. Thus, it is valid to regard u_{ref} as u. So, the transfer function can be approximated by the following equation.

$$\frac{T}{u_{ref}} \approx \frac{T}{u} = K\frac{-s^2 + (\beta - \alpha)}{s^2 + \alpha} \quad (4)$$

It is also valid to design a feedback controller for equation (4), if the closed loop pole is assigned near to the dominant system poles. As shown in equation, the pole is near the imaginary axis of s-domain, and the system is a non-minimum phase plant. The unknown parameters of (4), can be found by experimental identification. By measuring the oscillation period under position regulation control during single support phase, we can calculate α. By measuring the torque increment for ankle angle increment at steady state, we can also get $K(\beta-\alpha)/\alpha$. From the two equations, l and K can be identified. In addition, measuring a sinusoidal response for various input frequency is another method for verification. When the model is very complicated, it is actually hard to identify all the parameters. However, proposed model has an advantage in simple and easy parameter identification by experiment.

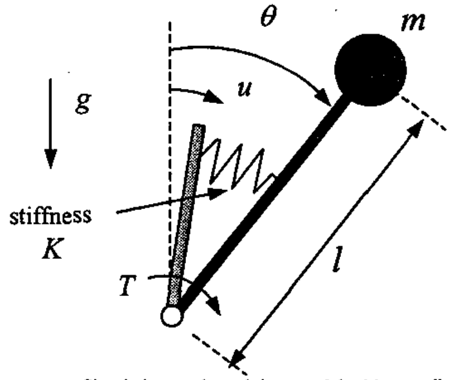

Figure 3. Simple inverted pendulum model with compliant joint

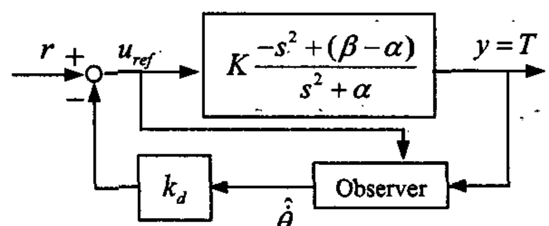

Figure 4. Block diagram of damping controller

B. Design of Damping Controller

Even though the system is a lightly damped system, we can increase its damping ratio using the following feedback law as shown in Fig.4.

$$u_{ref} = r - k_d\hat{\dot{\theta}} \quad (5)$$

where r is the command input of ankle joint.

With this damping controller, we can reduce the oscillatory motion induced by the external force when the PD position control is applied at the ankle joint.

From (1),(2),(4),(5), the following transfer function is derived:

$$\frac{\theta(s)}{r(s)} = \frac{K}{ml^2s^2 + k_dKs + (K - mgl)} = \frac{\frac{K}{ml^2}}{s^2 + 2\xi\omega_n s + \omega_n^2} \quad (6)$$

We can assign the damping ratio freely and the oscillatory motion can be suppressed effectively by changing k_d gain in the following equation.

$$k_d = 2\frac{\sqrt{ml^2(K-mgl)}}{K}\xi \tag{7}$$

The steady state value of the transfer function in (6) is

$$\lim_{s\to 0}\frac{\theta(s)}{r(s)} = \frac{K}{K-mgl} \tag{8}$$

and it is independent of k_d gain.

In (5), $\hat{\theta}$ should be calculated from the following observer equation.

$$\dot{w} = -L_o w - (L_o^2 + \alpha)(y + Ku) + K\beta u, \tag{9}$$

$$\hat{\theta} = \frac{1}{K}w + \frac{L_o}{K}(y + Ku) \tag{10}$$

where L_o is the observer pole.

For a practical implementation of the damping controller, the compensator transfer function in Fig.5 is derived from (4), (5), (9), (10).

$$K_c(s) = p_c\frac{s+p_b}{s+p_a} \tag{11}$$

with $p_a = \dfrac{L_o + (\beta-\alpha)k_d}{1+k_d L_o}$, $p_b = -\dfrac{\alpha}{L_o}$, $p_c = \dfrac{k_d L_o}{K(1+k_d L_o)}$

Therefore, increasing damping ratio in the light damped system can be regarded as making the simple first order polynomial compensator that stabilizes the torque oscillation. The damping controller can be applied to the pitch and roll axes of the ankle with different stiffness.

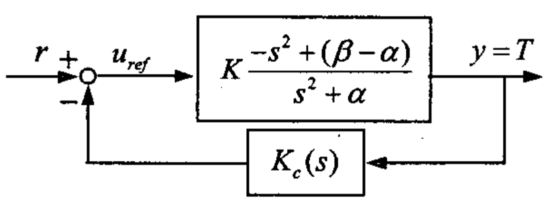

Figure 5. Block diagram of practical damping controller

C. Experimental Verification of Damping Controller

Fig.6 shows the experimental result of the proposed damping controller during single support phase. When only PD control is applied to the ankle, it does not decay the oscillation caused from external torque. However, with the damping controller, the oscillation decays out within 0.8 second. In the compensator, assigned observer pole L_o is 6 rad/s and damping ratio ξ is 0.707. This compensator works as a basic controller during single support phase of biped walking. The effectiveness of the proposed controller is described in section V. The experimental results for the proposed damping controller can achieve stable walking.

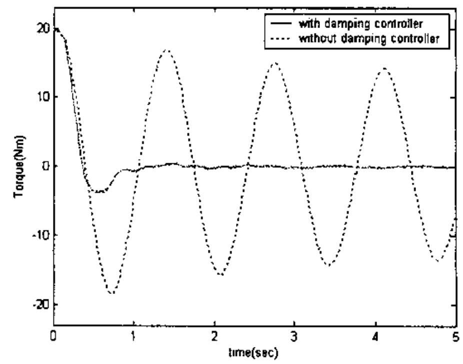

Figure 6. Time response of measured torque (Experimental result)

IV. Landing Control

A. Landing Orientation Controller of Ankle Joint

When a biped robot is walking by a prescribed walking pattern, the landing angle of the swing foot may be different from the prescribed landing angle. Moreover, the sole may not have perfect contact with the ground after landing. This can destabilize the robot. In the previous section, it is assumed that the sole is in perfect contact with the ground while the damping controller is applied. In order to enable the perfect contact, a landing orientation controller is implemented before damping controller is applied. It is known that a landing orientation controller can suppress instability and reduce impact [23]. From the viewpoint of the ankle position control, the essence of this landing orientation controller is somewhat different from damping controller that is described in section III.B. The damping controller tries to maintain its position against the external force. However, the compliance of the required landing orientation controller should be soft enough that position is shifted by external force easily. In the landing orientation controller of KHR-1, the ankle acts as the soft compliance that manages fast and stable ground contact without bouncing the foot off the ground. The reference angle of the ankle is controlled by the following equation in order to have the damping coefficient C_L and stiffness K_L for a measured torque T.

$$u_{ref}(s) = r + \frac{T(s)}{C_L s + K_L} \tag{12}$$

where C_L and K_L are tuned to provide the enough back drivability around the ankle pivot during single support phase.

B. Landing Position Controller

Prescribed walking patterns for the foot and the hip are shown in Fig.7 and Fig.8. The coordinate X, Y, Z are the sagittal, frontal, and vertical direction respectively. During single support phase, the position of swing foot moves along X-axis and Z-axis, and the position of supporting foot is fixed on the ground. Landing of a swing foot makes the transition to the double support phase. During double support phase, the position of both feet are fixed, but the hip position is free to move. Next transition to single support phase occurs when the heel leaves the ground. The prescribed walking patterns are made up of these phases and transitions. However, the actual landing time of the foot may be different from the prescribed landing time when the robot walks on an uneven terrain. When the actual landing occurs before the prescribed time, the use of the prescribed walking pattern without modification may cause undesirable effects. For example, if the position reference of the landing foot moves forward along X-axis, the relative movement between the two feet will induce a vibration of the ankle during the next heel-off phase. In addition, the stretching of landing foot along Z-axis also causes a landing impact at that time. In order to solve these problems, a landing position controller is implemented to prevent the movement of the swing foot along the X-axis and the Z-axis during unexpected landing [1,17]. Moreover, the landing position controller lengthens the stride on the next swing phase by the amount of loss, and slowly stretches the foot after the landing is fully completed. By this modification of the feet position and the recovery of stride, the robot can walk stably at a given speed. The overall block diagram for dynamic walking control is shown in Fig. 9. Landing orientation controller is applied on the swing foot during landing and damping controller is applied on the supporting foot after landing. In the diagram, landing position controller modifies the prescribed position of the swing foot when the foot touches the ground earlier than its prescribed time.

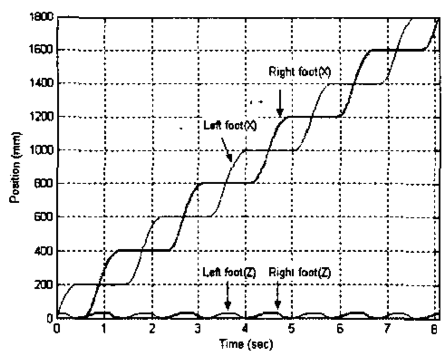

Figure 7. Prescribed trajectories of foot position

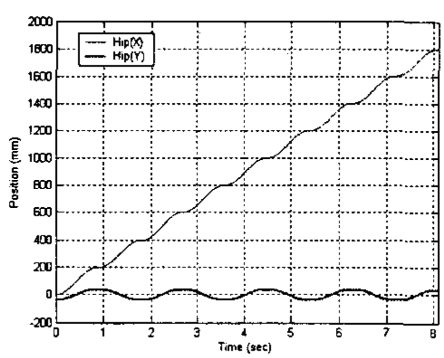

Figure 8. Prescribed trajectories of hip position

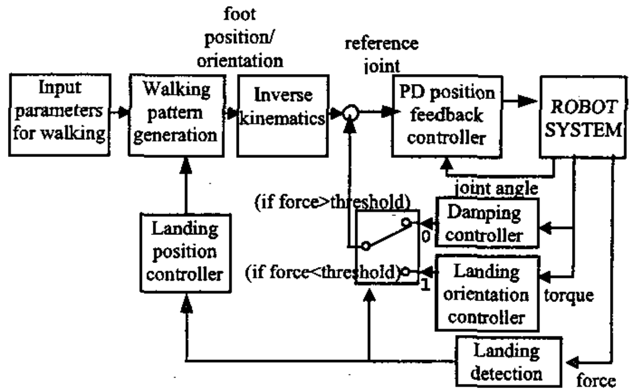

Figure 9. Block diagram of dynamic walking control

V. WALKING EXPERIMENT

In order to verify the performance of the proposed controller, walking experiment was performed at steady state. In our walking experiment, the exact solution for walking pattern was not solved because the focus is implementation of online controllers. Instead of designing the reference ZMP patterns, hip trajectories are simplified into function for easy tuning in real experiment. The prescribed trajectories of foot and hip positions are shown in Fig. 7 and Fig. 8 respectively. In the figures, the step length is 200 mm and the step period is 0.9 sec. The hip height is kept at a constant height and the orientation of the sole is kept parallel to the floor. With the proposed controllers and the trajectories in Fig. 7 and Fig. 8, stable walks could be achieved successfully. Fig. 10 represents the experimental results. In figure, the measured ZMP is inside the stable region. Measured normal forces are shifted periodically from one leg to the other. Fig. 11 shows photographs of KHR-1 walking on a treadmill.

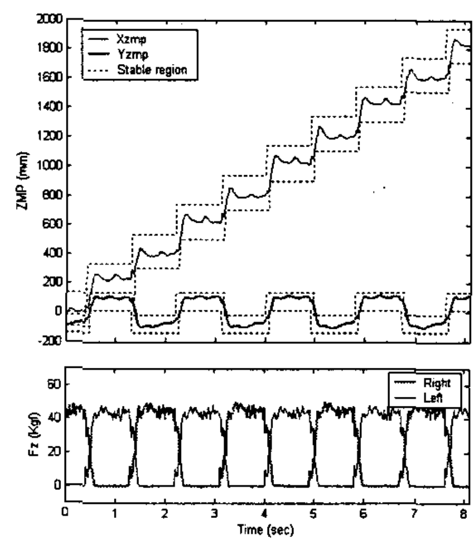

Figure 10. Measured ZMP and force

VI. CONCLUSION

In this paper, we have described the method to realize the dynamic walking for KHR-1 based on three controllers. The contributions of our paper are as follow:

1) We noticed that the ZMP error occurred due to lack of damping when we performed a position control during single support phase. So the simple inverted pendulum model with compliant joint was proposed for the basis of a controller design to correct for the ZMP error. Proposed model has an advantage in easy parameter identification by experiment.

2) From this model, damping controller was designed and its performance was evaluated by experiment. After the damping term was applied by damping controller, the inherent oscillation was damped.

3) Landing orientation controller and landing position controller were presented. These controllers were implemented to insure smooth and stable foot to ground interaction during landing.

4) The effectiveness of the whole control method was confirmed by the walking experiment.

As of the writing of this paper, stable walking of 1 km/h could be realized with the step length of 250 mm and step period of 0.9 sec. In order to increase the walking speed, the optimized trajectory planning and the robust stabilization scheme using orientation sensor will be required.

ACKNOWLEDGMENT

This work was partly supported by the Korea Science and Engineering Foundation (KOSEF) through the Human-friendly Welfare Robot System Engineering Research Center at KAIST, and Brain Korea 21 fund.

REFERENCES

[1] K. Hirai, M. Hirose, Y. Haikawa, and T. Takenaka, "The development of honda humanoid robot," *Proc. of Int. Conf. on Robotics and Automations*, Leuven, 1998, pp. 1321-1326.

[2] K. Nishiwaki, T. Sugihara, S. Kagami, F. Kanehiro, M. Inaba, and H. Inoue, "Design and development of research platform for perception-action integration in humanoid Robot: H6," *Proc. Int. Conf. on Intelligent Robots and Systems*, Takamatsu, 2000, pp. 1559-1564.

[3] Y. Sakagami, R. Watanabe, C. Aoyama, S. Matsunaga, N. Higaki, and K. Fujimura, "The intelligent ASIMO: System overview and integration," *Proc. Int. Conf. on IROS*, 2002, pp. 2478-2483.

[4] J. Yamaguchi, A. Takanishi, and I. Kato, "Development of a biped walking robot compensating for three-axis moment by trunk motion," *Proc. Int. Conf. on Intelligent Robots and Systems*, 1993, pp. 561-566.

[5] Q. Huang, K. Yokoi, S. Kajita, K. Kaneko, H. Arai, N. Koyachi, and K. Tanie, "Planning walking patterns for a biped robot," *Trans. on Robotics and Automation*, vol. 17, no. 3, 2001, pp. 280-289.

[6] K. Nagasaka, H. Inoue, and M. Inaba, "Dynamic walking pattern generation for a humanoid robot based on optimal gradient method." *Proc. Int. Conf. on Systems, Man, and Cybernetics*, 1999, pp. 908 -913.

[7] S. Kajita, F. Kanehiro, K. Kaneko, K. Fujiwara, K. Yokoi, and H. Hirukawa, "Biped walking pattern generation by a simple three-dimensional inverted pendulum model," *Advanced Robotics*, vol. 17, no. 2, 2003, pp. 131-147.

[8] H. O. Lim, Y. Yamamoto, and A. Takanishi, "Stabilization control for biped follow walking," *Advanced Robotics*, vol. 16, no. 4, 2002, pp. 361-380.

[9] K. Yokoi, F. Kanehiro, K. Kaneko, K. Fujiwara, S. Kajita, and H. Hirukawa, "A honda humanoid robot controlled by AIST software," *Proc. Int. Conf. on Humanoid Robots*, Tokyo, 2001, pp. 259-264.

[10] Napoleon, S. Nakaura, and M. Sampei, "Balance control analysis of humanoid robot based on ZMP feedback control," *Proc. Int. Conf. on Intelligent Robots and Systems*, Lausanne, 2002, pp. 2437-2442.

[11] M. Gienger, K. Löffler, and F. Pfeiffer, "Walking control of a biped robot based on inertial measurement," *Proc. of IARP Int. Workshop on Humanoid and Human Friendly Robotics*, Tsukuba, 2002, pp. 22-29.

[12] K. Yokoi, F. Kanehiro, K. Kaneko, K. Fujiwara, S. Kajita, and H. Hirukawa, "Experimental study of biped locomotion of humanoid robot HRP-1S," *Experimental Robotics VIII*, B. Siciliano and P. Dario (Eds.), Springer-Verlag , 2003, pp. 75-84.

[13] S. Kajita, K. Yokoi, M. Saigo, and K. Tanie, "Balancing a humanoid robot using backdrive concerned torque control and direct angular momentum feedback," *Proc. Int. Conf. on Robotics and Automation*, Seoul, 2001, pp. 3376-3382.

[14] S. Kagami, F. Kanehiro, Y. Tamiya, M. Inaba, and H. Inoue, "Autobalancer: an online dynamic balance compensation scheme for humanoid robots," *Proc. of 4th Int. Workshop on Algorithmic Foundations of Robotics*, Hanover, NH, 2000, pp. 329-340

[15] M. Vukobratovic, B. Borovac, D. Surla, and D. Stokic, *Biped locomotion : dynamics, stability, control and application*, Springer-Verlag, 1990.

[16] T. Sugihara and Y. Nakamura, "Whole-body cooperative balancing of humanoid robot using COG Jacobian," *Proc. Int. Conf. on Intelligent Robots and Systems*, Lausanne, 2002, pp. 2575 -2580.

[17] Q. Huang, K. Kaneko, *et al.*, "Balance control of a biped robot combining off-line pattern with real-time modification," *Proc. Int. Conf. on Robotics and Automation*, San Francisco, CA, 2000, pp. 3346-3352.

[18] Napoleon, S. Nakaura, and M. Sampei, "Balance control analysis of humanoid robot based on ZMP feedback control," *Proc. Int. Conf. on Intelligent Robots and Systems*, Lausanne, 2002, pp. 2437- 2442.

[19] J. H. Kim, S. W. Park, I. W. Park, and J. H. Oh, "Development of a humanoid biped walking robot platform KHR-1 – initial design and its performance evaluation," *Proc. of IARP Int. Workshop on Humanoid and Human Friendly Robotics*, Tsukuba, 2002, pp. 14-21.

[20] J. H. Kim, I. W. Park, and J. H. Oh, "Design of lower limbs for a humanoid biped robot," *Int. J. Human-friendly Welfare Robotic Syst.*, vol. 2, no. 4, 2002, pp. 5-10.

[21] J. E. Pratt, *Exploiting Inherent robustness and natural dynamics in the control of bipedal walking robots*, PhD Thesis, MIT, 2000.

[22] J. H. Kim and J. H. Oh, "Torque Feedback Control of the Humanoid Platform KHR-1," *Proc. of 3rd IEEE Int. Conf. on Humanoid Robots*, Karlsruhe and Munich, Germany, Oct. 1-3, 2003

[23] J. H. Park and H. Chung, "Hybrid control for biped robots using impedance control and computed-torque control," *Proc. Int. Conf. on Robotics and Automation*, Detroit, MI, 1999, pp. 1365-1370.

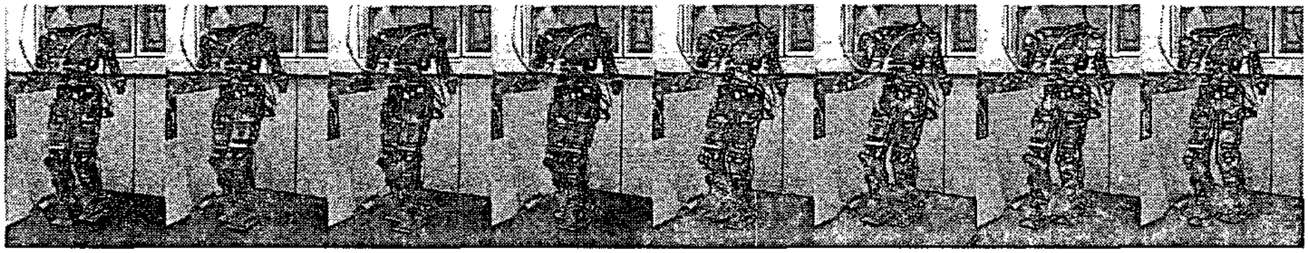

(a) 0.0 sec. (b) 0.2 sec. (c) 0.4 sec. (d) 0.6 sec. (e) 0.8 sec. (f) 1.0 sec. (g) 1.2 sec. (h) 1.4 sec.

Figure 11. Photo sequence of the walking experiment